

# Modeling step bunching formed on vicinal GaAs(001) annealed in AsH<sub>3</sub> and hydrogen ambient

K. Hata and H. Shigekawa

*Institute of Materials Science and Center for Tsukuba Advanced Research Alliance, University of Tsukuba, Tsukuba 305, Japan*

T. Okano

*Institute of Industrial Science, The University of Tokyo, 7-22-1 Roppongi, Minato-ku, Tokyo 106, Japan*

T. Ueda and M. Akiyama

*Semiconductor Technology L Co. Ltd., 550-5 Higashi-Asakawa, Hachioji, Tokyo 193, Japan*

(Received 5 August 1996)

A detailed analysis of the surface morphology of step bunching formed by annealing in AsH<sub>3</sub> and hydrogen has been carried out on substrates with various miscut directions. The results show that branches, by which we refer to step bunchedings that do not run in the substrate miscut direction, form on most of the substrates and for most of the annealing conditions, suggesting that they have a relatively low free energy and compose an intrinsic component of this step bunching. Also these branches are not randomly located on the surface but have a strong tendency to align side by side. In order to understand these experimental results, we propose a qualitative model designated as the "chain reaction model." This model is founded on the fact that during annealing steps can only move by exchanging step-edge atoms with other steps. By this model we can explain the main characteristics of this step bunching: why the step bunching does not grow infinitely in size and why branches have a strong tendency to align side by side. [S0163-1829(97)07311-6]

## I. INTRODUCTION

Step bunching is a phenomenon in which the surface breaks up into regions with high step densities and regions with little or no steps. This phenomenon itself was known long ago,<sup>1-4</sup> but until recently it was believed that step bunching is a rare phenomenon, and is not so important to our understanding of the characteristics of steps. Recent reports from many researchers showing the formation of step bunching on many systems has overturned this concept, and gradually it became recognized that step bunching is not at all rare and uncommon, but is a phenomenon that occurs on many systems and reflects the true nature of steps.

Step bunchedings are observed on almost every kind of surface, including compound materials,<sup>5-7</sup> metals,<sup>8-10</sup> stressed interfaces,<sup>11-14</sup> semiconductors, sputtered surfaces,<sup>15</sup> epitaxially grown surfaces,<sup>16</sup> annealed surfaces,<sup>17-20</sup> and so on. Also the believed origin of these step bunchedings ranges from pinning by impurities<sup>21,22</sup> to electromigration,<sup>23,24</sup> coexistence of different reconstructions,<sup>25,26</sup> faceting,<sup>8</sup> and absorbates.<sup>27,28,15</sup> This shows that step bunching is a very popular and complicated phenomenon to understand and it is no wonder that many experimentalists and theorists have started to pick it up as a subject for research.

Particularly, one can realize the importance of step bunching formed on a GaAs substrate by recognizing that GaAs is the material in which most of the nanodevices are fabricated, and indeed, the size of step bunching formed on this surface is on the scale of nanometers. Several step bunchedings form on GaAs. They form on the (110) (Refs. 29-32) and high indexed surfaces such as (311).<sup>33-35</sup> Also several types of step bunchedings are reported to form on the (001) surface.<sup>16,36,37</sup> By annealing layers grown by molecular beam epitaxial in ultrahigh vacuum, the surface transforms from an

As-rich to a Ga-rich configuration. Step bunching forms when two Ga-rich reconstructions,  $c(2\times 8)$  and  $c(2\times 6)$ , coexist on the surface.<sup>36</sup> Also on the As-rich (001) surfaces, step bunching forms. The prime feature of step bunching that forms on As-rich vicinal GaAs(001) is that it only occurs when AsH<sub>3</sub> and hydrogen are exposed to the surface.<sup>37</sup> Therefore it is natural that this step bunching was first observed on layers grown by metalorganic chemical vapor deposition (MOCVD).<sup>16</sup> Since then, several groups have researched the characteristics of this step bunching,<sup>38-47</sup> studying the influence of growth conditions and substrates on the surface morphology and dynamics of step bunching. At first, it was believed that this step bunching originates from MOCVD epitaxial growth itself; however, we have shown previously that similar step bunchedings also form on surfaces only annealed in AsH<sub>3</sub> and hydrogen atmosphere.<sup>37</sup> Further research showed that during the evolution of this step bunching (on a substrate misorientated in the [100] direction), additional step bunchedings (branches) that do not run in the miscut direction of the substrate spontaneously appear.<sup>17</sup> Another prime feature of this step bunching is that it does not grow infinitely in size with annealing time, but after it evolves into a particular size, its development stops, and surface morphology remains unchanged.

In this paper we report more detailed experimental research concerning the appearance of these branches on substrates with various miscut directions and model the bunching process. We will show that branches form on most of the substrates and for most of the annealing conditions, suggesting that they have a relatively low free energy and comprise an intrinsic component of this step bunching. If we classify directions [100],  $[1\bar{1}0]B$ , and  $[110]A$  as group I, and  $[210]$  and  $[2\bar{1}0]$  as group II, facets of branches observed on group I substrates have the azimuth of group II, and vice versa.

Moreover, careful analysis of the scanning tunneling microscopy (STM) images showed that these branches are not randomly distributed on the surface, but have a strong tendency to align side by side. We will propose a model designated as the “chain reaction model” which explains the prime characteristics of this step bunching. This model is based on the fact that during annealing steps can only move by exchanging step-edge atoms with other steps and that step bunching occurs only when an upward mass transfer across the step edge exists. Under these conditions, we will model the bunching process, showing that whether the bunching continues to grow or not is determined by a competition of two diffusion processes. Diffusion process I causes large step buncings to grow larger at the expense of smaller step buncings while diffusion process II does not. It is easy to see that while the size of the step bunching is small, diffusion process I is easily completed, though it rapidly becomes difficult as the size of the step bunching becomes larger. Thus we assume that a turning point exists, and diffusion process II starts to take place. In such a situation, step bunching stops to grow in size once it reaches a particular stage. This agrees with the results of experiments. Moreover, by a side effect, branches align side by side in a fashion consistent with the STM images.

## II. EXPERIMENT

### A. Substrates

We used five types of vicinal substrates miscut toward  $[100]$ ,  $[110]A$ ,  $[1\bar{1}0]B$ ,  $[210]$ , and  $[2\bar{1}0]$  with a miscut angle of  $2.0^\circ$ . The miscut angle was fixed at  $2.0^\circ$  in this study. The miscut angle is an important parameter that does influence the morphology and size of step bunching. Its influence on the surface morphology of step bunching has been studied by other groups in both the steeper<sup>41</sup> and shallower angle region.<sup>42</sup> All of the substrates we used in this study were cut out from the same GaAs rod. To impart the necessary conductivity to carry out STM observations, the substrates were Si doped with a carrier concentration of  $4 \times 10^{17} \text{ cm}^{-3}$ . This is lower than the usual carrier concentration, which is on the order of  $10^{18} \text{ cm}^{-3}$ . These Si impurities have the potential to influence the morphology of step bunching; in fact, they can work as a Frank impurity and be the direct cause of the observed step bunching.<sup>48–52</sup> Indeed step edges of vicinal GaAs(001) with a carrier concentration above  $3 \times 10^{18} \text{ cm}^{-3}$  are reported to become rough, because Si dopants create kinks in the dimer vacancy rows.<sup>53,54</sup> However, Fukui *et al.* has reported that carrier concentration of our order does not seriously affect the surface morphology.<sup>55</sup> They concluded this by comparing the surface morphologies of doped and nondoped substrates by atomic force microscopy (AFM), showing that there is no major difference in surface morphology between them. Therefore, we suppose that the surface morphology we observe does reflect the true nature of GaAs(001) annealed in AsH<sub>3</sub> and hydrogen ambient, and that doping is not the origin of the observed step bunching nor does it influence the observed surface morphology.

### B. Annealing procedure

The annealing process is quite similar to that of MOCVD growth; in fact, it is carried out in the same reactor used for MOCVD growth. The only difference between the annealing process and MOCVD growth is that the surface is not exposed to III species in the former; therefore no crystal growth takes place. Before annealing, first, the sample was cleaned by H<sub>2</sub>SO<sub>4</sub> dipping, followed by chemical etching in an H<sub>2</sub>SO<sub>4</sub>, H<sub>2</sub>O<sub>2</sub>, H<sub>2</sub>O; 4:1:1, solution. Approximately  $2 \mu\text{m}$  of the surface layers were removed by this etching process to obtain a surface free from contamination. After chemical etching, the substrate was introduced into the MOCVD reactor system, and was placed on a GaAs-coated carbon susceptor and annealed to the growth temperature by rf heating. The annealing temperature was monitored by a thermocouple inserted into the susceptor. The temperature was increased at a rate of approximately  $50^\circ\text{C}/\text{min}$  to the annealing temperature and kept constant. The total pressure during MOCVD growth was  $1.3 \times 10^4 \text{ Pa}$ , and the typical flow rates of AsH<sub>3</sub> and hydrogen were 40 and  $4000 \text{ s cm}^3$ ; therefore the partial pressure of As was approximately  $1.3 \times 10^2 \text{ Pa}$ . The partial pressure of As was not varied in this study. After the sample was annealed, the temperature was decreased at the rate of  $100^\circ\text{C}/\text{min}$  to room temperature. During cooling down the sample, it was exposed to AsH<sub>3</sub> and hydrogen to avoid surface roughening due to As desorption. After the sample was quenched to room temperature, it was placed in a nitrogen-purged transfer box and STM measurement was done as fast as possible.

### C. STM measurements

The STM used in this research is the commercial NanoScope II. The head of the STM was placed on a stack made by plates of iron and rubber, which itself was located on an air dumper vibration isolator. Also, the STM-controller current was taken from a stabilizer in order to get rid of electrical noise, and the ac power of the computer system was taken from a noise-cut transfer system. Care was taken to isolate the source of the controller current from other systems as much as possible. It is extremely difficult to obtain a good image of GaAs(001) by STM in air ambient; in general, observation by AFM is far more easy, however, occasionally we could obtain a very high resolution image. To the best of our knowledge, AFM images are somewhat more rough, therefore all of our observations shown here were carried out by STM. We used a tip fabricated by cutting an In-Pt (In 5%) wire by a nipper. Deterioration of the tunneling tip was the prime impediment to the efficiency of this experiment. Usually a single tip would last no more than 10 min, and we had to consume 10–20 tips before an STM image with high resolution could be obtained. This deterioration is believed to be due to the blunting of the tunneling tip caused by shaving the oxidized layer on the GaAs(001) surface. Occasionally a high-resolution image could be obtained and in such cases the tip had a longer lifetime than usual, sometimes, high-resolution observations with good reproducibility were possible for several hours on end. The tunneling current was in the range 0.9–3 nA, and the tunneling voltage in the range  $-1.8$  to  $-3.0 \text{ V}$ . The tunneling voltage and current in this

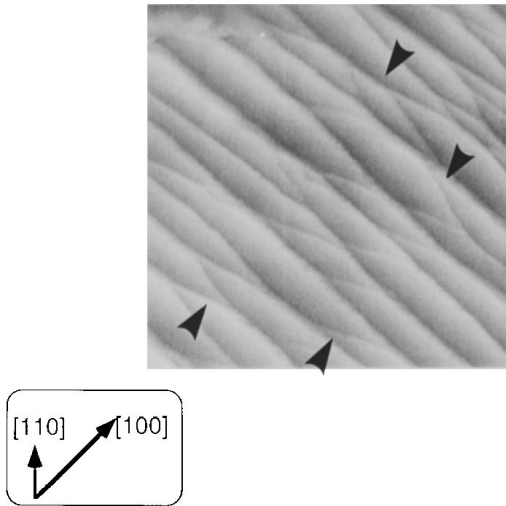


FIG. 1. A STM image of the surface of vicinal GaAs(001)-[100] $2^\circ$  annealed in AsH<sub>3</sub> and hydrogen at 700 °C for 10 min. Step bunching forms. Location where the branches align side by side is indicated by the arrows. Scale is 1000×1000 nm.

range did not affect the observed STM images. All of the images shown in this paper were taken in the constant current mode.

Since STM measurements were performed in air ambient, the GaAs surface is oxidized. It is not known what kind of disturbance this oxidized layer would cause; however, for Si(111) (Ref. 56) and GaAs(100) (Ref. 57) surfaces a single step is observed by AFM in air ambient. These results imply that a single-step corrugation remains even on an oxidized surface and is observable by STM, AFM. The thickness of the oxidized layer was estimated to be about 20 Å by ellipsometry measurement, which is in good agreement with the results of angle-resolved x-ray photoelectron spectroscopy measurements carried out by Whitehouse.<sup>58</sup>

### III. RESULTS

#### A. Existence of branches

A STM image of the surface of vicinal GaAs(001)-[100] $2^\circ$  annealed in AsH<sub>3</sub> and hydrogen at 700 °C for 10 min is displayed in Fig. 1. Periodical strips observed on the image running against the miscut direction represents facets composed of several monosteps generated by the miscut of the sample.<sup>37</sup> No or few steps exist between these facets and this region is supposed to be a (100) terrace. Step bunching has formed. Besides these facets the STM image shows additional step bunches (branches), which do not run in the miscut direction of [100], and connect two facets making the surface resemble a mesh. These branches are not monosteps but also represent facets composed of several monosteps. Branches do not run in arbitrary directions, but as Fig. 1 shows, they have a peculiar azimuth of  $\langle 210 \rangle$ ,  $\langle 2\bar{1}0 \rangle$ ,  $\langle 310 \rangle$ , and  $\langle 3\bar{1}0 \rangle$ . These branches were observed on all of the substrates and for most of the annealing conditions researched in this study. Although no statistical analysis had been carried out, once these branches form, their number seemed not to decrease on the surfaces annealed at high temperatures or longer times. These results are striking when one pays re-

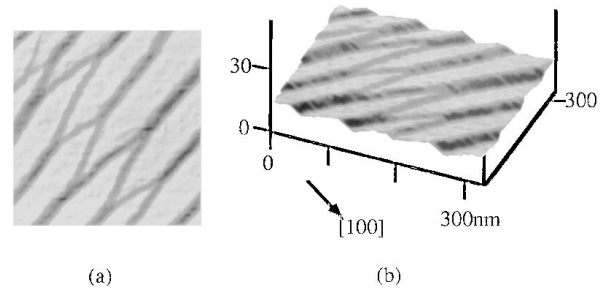


FIG. 2. Branches have a strong tendency to align side by side. As STM image of branches aligned side by side is shown in (a). (b) is a bird's eye view of (a).

spect to the surface energy. The morphology of the surface of a crystal will seek the shape that minimizes the sum total of the surface energy over the surface.<sup>59</sup> This means that extra steps are not favored because their existence would increase the total area of the surface, and one would expect that annealing the surface at high temperatures would make branches merge to decrease the area of the surface, though this was not observed. The strong tendency of branches with these peculiar azimuths to appear suggests the surface free energies of these facets are relatively low.<sup>60,61</sup>

#### B. Alignment of branches

Careful analyses of the STM images show that these branches are not randomly located on the surface, but have a strong tendency to align side by side. Such alignment of branches was observed frequently on the surface, as demonstrated in Fig. 1. Branches align on the line connected by the arrow. Most of the branches included in the alignment have facets with an azimuth of  $\langle 310 \rangle$  and  $\langle 3\bar{1}0 \rangle$ , while the facets of the side branches have azimuths of both  $\langle 210 \rangle$ ,  $\langle 2\bar{1}0 \rangle$  and  $\langle 310 \rangle$  and  $\langle 3\bar{1}0 \rangle$ . To illustrate this aspect more clearly, a closeup STM image and its three-dimensional perspective view showing the fashion of the alignment of branches is displayed in Fig. 2. Facets with azimuth of  $\langle 310 \rangle$  and  $\langle 3\bar{1}0 \rangle$  align alternatively. These branches split the main facet into two at the middle. Therefore, branches are not a monostep but are also a facet containing several steps. This fact is important when one attempts to model the bunching process; the proposed mechanism must be able to reconstitute the alignment of branches and the ways the facets split; thus we exclude models in which the development of step bunching is described by an exchange of single steps among facets, a mechanism that applies to step bunching formed on Si(111). Another set of STM images showing a wide region of the bunched surface is displayed in Fig. 3. In this figure, branches that we consider to be aligned are shown by real lines, while those that are not (single branches) are shown by dashed lines (the allocation of aligned or single is somewhat a matter of subjective choice) and Fig. 3(b) shows a histogram of the numbers of aligned branches versus single branches. It shows that there are three times more aligned branches than single branches. Also, in order to give more objective data, we have plotted all of the centers of the branches by a dot as shown in Fig. 3(c). It clearly shows that the distribution of the branches is not random, but there are many locations on the surface where branches have aligned

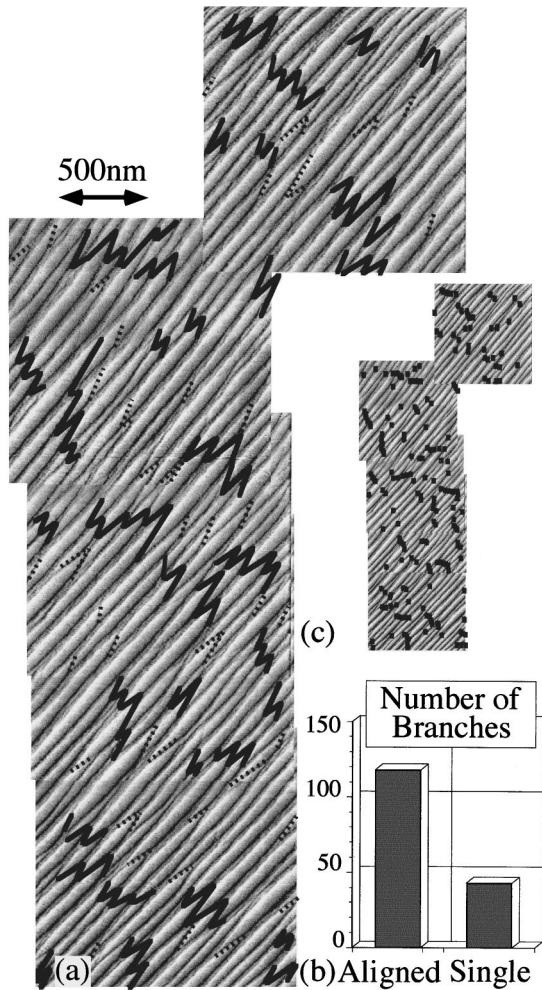


FIG. 3. An STM image of a wide range of surface of vicinal GaAs(001)-[100] $2^\circ$  annealed at  $600^\circ\text{C}$  with partial pressure of  $\text{AsH}_3$ , 1 Torr. Each STM image, represented as a box, is  $1500\text{ nm}$  square in size. In this figure, branches that we consider to be aligned are traced by solid lines, while those that are not (single branches) are shown by dashed lines. The allocation of aligned or single is somewhat a matter of subjective choice, though the same standard was applied for all branches. (b) A histogram of the numbers of aligned branches vs single branches counted from (a). (c) The same STM image of (a), where the center of the branches are plotted by a dot. These data show that the branches have a tendency to align up.

up. These data will give support to our insistence that branches have a strong tendency to align side by side.

### C. Branches on substrates with various miscut directions

We have shown that branches running against the  $\langle 210 \rangle$  and  $\langle 310 \rangle$  or  $\langle 2\bar{1}0 \rangle$  and  $\langle 3\bar{1}0 \rangle$  directions exist and line up on substrates miscut toward the  $[100]$  direction. This suggests that there exists a facet in these azimuth directions that has a relatively low surface free energy. This fact would naturally lead to the following questions: What would happen on substrates initially miscut in the  $\langle 210 \rangle$ ,  $\langle 310 \rangle$ ,  $\langle 2\bar{1}0 \rangle$ , and  $\langle 3\bar{1}0 \rangle$  directions? Would these branches disappear and a complete straight facet emerge, or will a similar branch appear again? If so, what kinds of branches would emerge? To address

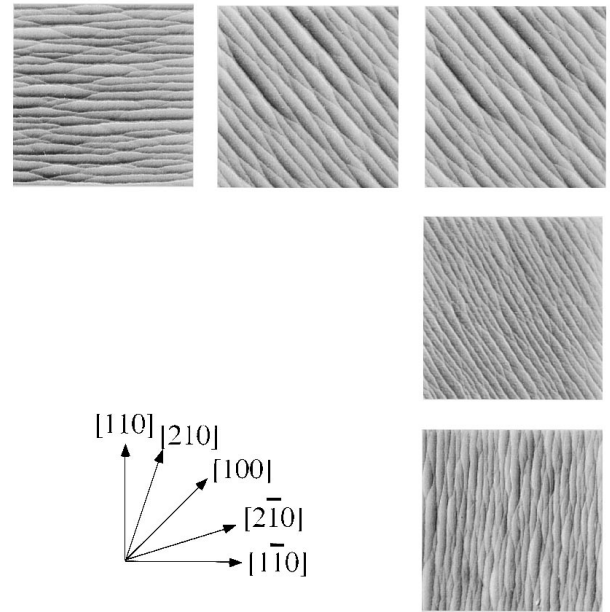


FIG. 4. Step bunching on substrates with various miscut directions. The displayed substrates were miscut in  $[210]$ ,  $[2\bar{1}0]$ ,  $[100]$ ,  $[1\bar{1}0]$ , and  $[110]$ . The miscut angle is  $2^\circ$ . Annealing conditions are the same,  $700^\circ\text{C}$  for 10 min, with  $\text{AsH}_3$   $1.3 \times 10^2$  Pa, except the substrate miscut in  $[1\bar{1}0]$  which was annealed at  $700^\circ\text{C}$  for 5 s with  $\text{AsH}_3$   $1.3 \times 10^1$  Pa. On all of the substrates branches form.

these questions we prepared substrates miscut in the  $[210]$ ,  $[2\bar{1}0]$ ,  $[110]_A$ , and  $[110]_B$  directions for  $2^\circ$ . These substrates, except  $[110]_B$ , were annealed in  $\text{AsH}_3$  and hydrogen ambient for 10 min at  $700^\circ\text{C}$ , the same process that results in step bunching for substrates miscut in the  $[100]$  direction. Note: the annealing condition of the substrate miscut in the  $[1\bar{1}0]_B$  direction is different from the others. Figure 4 shows STM images of these surfaces and substrates miscut in the  $[100]$  directions, which is displayed for comparison. Figure 4 clearly shows the formation of branches. Branches formed on every substrate researched in this study. At least, at some certain annealing conditions, in fact in most annealing conditions, on every substrate, branches are observed. These results strongly suggest that branches form a basic component of this step bunching. Figure 4 and Table I summarize these results, showing what kinds of branches are observed on each substrate. If we classify directions  $[110]_A$ ,  $[1\bar{1}0]_B$ , and  $[100]$  as group I and directions  $[210]$  and  $[2\bar{1}0]$  as group II, we notice that the facets of branches observed on group I substrates have the azimuth of group II, and vice versa. Seldom did a branch observed on group I substrates have a facet

TABLE I. List of the substrates with various miscut directions and the direction of branches observed on them.

Miscut direction of substrate	Directions of branches
$[110]$ group I	$\langle 210 \rangle, \langle 310 \rangle$ group II
$[210]$ group II	$\langle 100 \rangle, \langle 110 \rangle$ group I
$[100]$ group I	$\langle 210 \rangle, \langle 310 \rangle, \langle 3\bar{1}0 \rangle, \langle 2\bar{1}0 \rangle$ group II
$[2\bar{1}0]$ group II	$\langle 100 \rangle, \langle 110 \rangle$ group I
$[1\bar{1}0]$ group I	$\langle 2\bar{1}0 \rangle, \langle 3\bar{1}0 \rangle$ group II

with the azimuth of group I. To illustrate, on a substrate miscut in the  $[100]$  direction, no branches had a facet with azimuth of  $\langle 110 \rangle$  or  $\langle \bar{1}\bar{1}0 \rangle$ . This means that the angles between the main facets and branches were always in the region of  $20^\circ$  to  $30^\circ$ , a somewhat surprising result when one considers the total area of the surface; a group I branch on a group I substrate would have a smaller total surface area than a group II branch on a group I substrate, though this is not what was observed.

#### IV. DISCUSSION

##### A. Existence of branches

We have stated in the previous sections that we believe the observed branches compose an intrinsic part of this step bunching. However, it is possible that these branches are induced by a small miscut against the net-misoriented direction (small miscut). A small miscut against the net-misoriented direction refers to the deviation of the real miscut direction from the intended miscut direction, e.g., a sample referred to here as a substrate with a miscut direction of  $[110]$ , is not, actually, miscut in the exact  $[110]$  direction and there is always a small deviation. This deviation will produce kinks in the steps, and the observed branches may be nothing but kinks stacked in a pile. In such a case, the direction of the branches that are the majority in number should reflect the direction of the small miscut; e.g., when the substrate is net-miscut in the  $[001]$  direction, and the small miscut is in the  $[110]$  direction, the number of branches running against the  $\langle 210 \rangle$  and  $\langle 310 \rangle$  directions (branches that reflect the small miscut clockwise to the net-miscut) should dominate the number of those running against the  $\langle \bar{2}10 \rangle$  and  $\langle \bar{3}10 \rangle$  directions (branches that reflect the small miscut counterclockwise to the net-miscut). Such a domination of one type of branch was not observed, and the numbers of the two types of branches (clockwise and counterclockwise branches) were not seriously different, meaning that these branches are not organized by a small miscut.

If the facets of the branches have a relatively low surface free energy, and a strong tendency to emerge on the surface, naturally other research should have observed these facets before. Here we will enumerate studies that report the appearance of facets with the same azimuth as the branches.<sup>59–66</sup> Facets with the  $\langle 210 \rangle$  and  $\langle 310 \rangle$  azimuths were observed to spontaneously appear on extended facets of molecular-beam-epitaxy deposited GaAs(001).<sup>59</sup> Moreover, gratings with  $[210]$  and  $[120]$  azimuths were used to show the high stability of these facets, and the Miller index of these facets was determined to be  $(216)$ .<sup>60</sup> Also superior crystal-growth properties have been observed on the  $(311)$  surface rather than on  $(001)$  and  $(111)$  surfaces.<sup>62</sup> Under certain growth conditions the side wall of a quantum dot and wire develops into a  $\{211\}$  facet.<sup>63–65</sup> Also, step bunching similar to ours has been observed on GaAs(311)A surfaces grown by MOCVD.<sup>66</sup> All of the facets with  $\langle 210 \rangle$ ,  $\langle \bar{2}\bar{1}0 \rangle$ , and  $\langle 310 \rangle$  azimuths observed so far appeared on layers grown by epitaxial growth or structures artificially fabricated. Here, we have shown that these facets appear even on annealed surfaces. The strong tendency of these facets to emerge even on annealed surface means that their surface energies are low. However, at this stage, the reason that these facets are so

stable is not understood. Further studies are required to clarify why these particular facets are highly stable. Especially high-resolution STM studies are desired to establish an atomic model of the structure of the facets. Since our STM observations do not have an atomic resolution we will not lay down any structure model for the facet in this paper, instead we only mention some possible mechanism that may be related to the observed stability of branches. Benisty, Bockenhoff, and Taineau<sup>59</sup> attempted to explain the high stability of these facets by an interaction between the “step-kink” structure<sup>67</sup> and the reconstructed “missing dimmer” terrace structure.<sup>68</sup> Another possible mechanism is the recently observed short-range kink-kink repulsion, which affects the kink-kink length and thus may have some role in determining the peculiar azimuth of these facets.<sup>69</sup>

##### B. Modeling step bunching and the alignment of branches

In this section we will propose a simple model designated as the “chain reaction model” in order to explain both the observed alignment of branches and the saturation of the size of step bunching. This model is based on some fundamental characteristics of step dynamics during annealing. However, this is valid only when desorption of atoms from the surface can be neglected. Indeed desorption of atoms from the surface is a possible formation mechanism of this step bunching. We concluded that desorption can be neglected because of an experiment carried out by Ohkuri *et al.*<sup>70</sup> They prepared two vicinal GaAs(001) surfaces masked with a  $\text{SiN}_x$  line and space pattern. Then one of the substrates was thermally annealed in  $\text{AsH}_3$  and  $\text{H}_2$  ambient at  $800^\circ\text{C}$  for 30 min (a longer annealing time and higher annealing temperature than our experimental conditions) while the other was not. Then they etched off the masked  $\text{SiN}_x$  and compared the depth of the trenches of the two substrates by atomic force microscopy. The results show that even under these severe annealing conditions in which desorption is far more likely to occur than our experiments, only two or so monolayers of GaAs desorbed from the surface during the annealing process. The height of two or so monolayers ( $\sim 5 \text{ \AA}$ ) is lower than the height of the facet of step bunching ( $20\text{--}30 \text{ \AA}$ ), thus we conclude that desorption is negligible.

Before laying down the details of this model, first we will comment on some fundamental properties of step dynamics during annealing. During annealing, steps can only move by exchanging step-edge atoms with other steps. By estimating the total balance between the number of atoms detaching from and incorporating into a step edge per unit time, we can determine the velocity of the step as a set of different differential equations (time evolution equation), which describes the evolution of the step system.<sup>71</sup> The Schwoebel effect<sup>72</sup> is considered in the detachment and incorporation processes. The time evolution equation shows that whether a step bunching or a regular monostep array forms is determined by the sign of

$$\alpha_{\text{out}}\beta_{\text{in}} - \beta_{\text{out}}\alpha_{\text{in}} \quad (\text{DDI factor}), \quad (1)$$

where  $\alpha_{\text{out}}$  and  $\beta_{\text{out}}$  are the probabilities of the step-edge atom to detach to the lower and upper boundary terraces, and  $\alpha_{\text{in}}$  and  $\beta_{\text{in}}$  are the probabilities of a diffusing atom approaching a step edge from the lower and/or upper terraces to

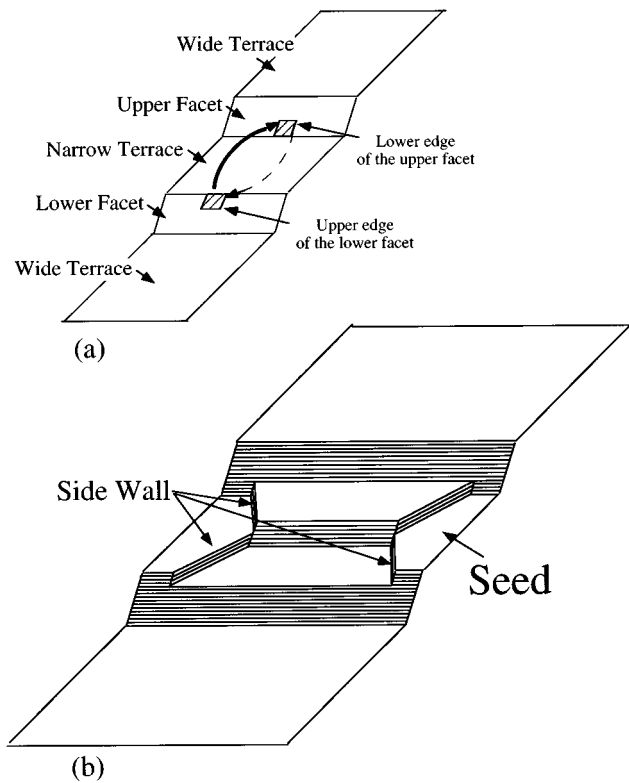


FIG. 5. Schematic of the system considered in the chain reaction mechanism. (a) is a schematic of the initial system. (b) shows the formation of a seed.

be incorporated into the step edge, respectively. When the sign of the DDI factor is positive, exchange of step-edge atoms with other steps functions as a repulsive interaction between steps, and consequently a train of monosteps evolves into a regular array of steps. On the other hand, when the DDI factor is negative, the exchange works as an attractive interaction between steps, and consequently step bunching occurs.<sup>71</sup> Since  $\alpha_{out}\beta_{in}$  and  $\beta_{out}\alpha_{in}$  indicate the upward and downward mass transfer across the step edge, step bunching occurs when there exists an upward net mass transfer across the step edge. This situation is most easily realized by a case in which the step-edge atoms detach more easily from the upper terrace than from the lower terrace, a condition initially considered by the classical paper of Schwoebel and Shipsey.<sup>72</sup> [They considered the  $\alpha_{in}=1$  and  $\beta_{in}=1$  case. Equation (1) is a more generalized result considering anisotropic incorporation.] Adopting the situation considered by Schwoebel and Shipsey, i.e., neglecting the anisotropy in the incorporation process, does not lose any generality, thus we will consider that case in the following for simplicity.

Now let us consider a system composed of three terraces, the two sides being rather wide while the middle one is narrower, and two facets between the terraces, as shown schematically in Fig. 5. By considering the above-mentioned net flow of atoms induced by the Schwoebel effect, one can see that there exists a net flow of atoms from the upper edge of the lower facet to the lower edge of the upper facet. Consequently, the steps at the upper edge of the lower terrace would recede (move inward in the schematic) while the steps at the lower edge of the upper terrace would advance (move

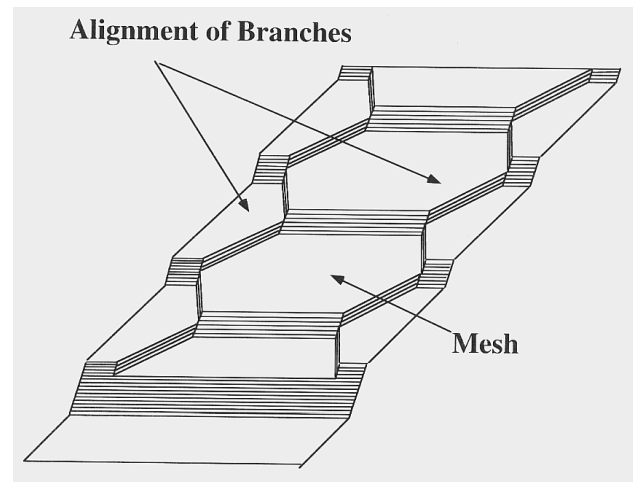


FIG. 6. Schematic showing how branches align by the chain reaction model. Branches in the schematic align in the same way they really do. See the STM image of Fig. 2.

outward). If this process proceeds, finally these steps will collide and form a new facet at the middle of the narrow terrace. It is natural to suppose that the side wall steps, which are an essentially by-product of this process, run in a direction with a relatively low surface free energy (the direction of the branches). So we are left with a structure shown schematically in Fig. 5. This structure will be nominated "a seed" and the process to form it a "growth process." Indeed, this seed structure is frequently observed on the surface. Similarly, the next steps can move inward and outward as before, and again collide at the middle of the terrace forming a larger facet; however, there is a difference compared to the aforementioned process; this time the atoms diffusing across the middle terrace have to diffuse over the newly created facet, which would be a rather stumbling process. Therefore, it would become increasingly difficult to finish this growth process as the middle facet grows in size; however, if it does, and all of the possible growth processes complete (within the system under consideration), we are left with two wide terraces and one large facet; indeed this is nothing but the usual bunching process. Large terraces grow wider at the expense of narrow terraces. If this bunching process continues to complete consuming other narrow terraces on the surface, step bunching will keep on growing, though this is not what is observed. It is well established that step bunching does not grow infinitely in size with annealing time but after it evolves into a particular size its development stops and surface morphology remains unchanged.<sup>17-19,37</sup> Thus we assume that the growth process is completed when the newly created facet is small, though as the facet grows in size quickly it becomes difficult for this process to complete because the diffusing atoms have to cross over many steps, and instead of completing this process, a new seed forms on the adjacent terrace, and this seed in turn acts on its adjacent terrace forming another seed on it, and so on. This is like a chain reaction, a seed on a terrace induces another seed on its adjacent terrace. In that case, we are left with a structure schematically shown in Fig. 6. As Fig. 6 shows branches align side by side in a fashion that exactly corresponds to the STM images (compare the right side of Fig. 6 to the STM image shown in Fig. 2), branches split the main facets into two at

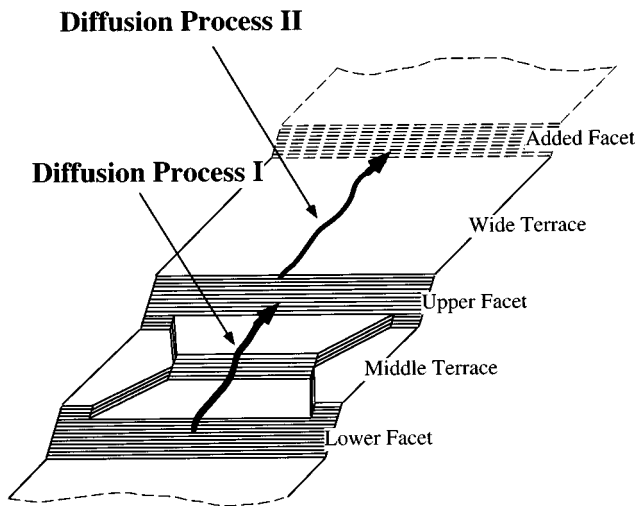


FIG. 7. Schematic showing the new system considered to consult whether the growth process completes or the chain process starts. The new system is based on Fig. 5(b), a new facet is added to the upper side. The two diffusion processes are indicated by the arrows.

the middle point, and two types of branches align alternatively, e.g., branches having facets with the azimuth of  $\langle 310 \rangle$  and  $\langle \bar{3}10 \rangle$  in the STM image. Moreover, even if this chain reaction goes on endlessly the number of the facets does not change (see Fig. 6), in other words, once the chain reaction starts to take place, the growth of step bunching stops. If this chain reaction mechanism is practiced, the surface of the bunched structure should be basically composed of a mesh-like structure shown in Fig. 6. The wide region STM image of Fig. 3 clearly shows that the surface regions where the alignment of branches are observed can be considered as aggregates of these meshlike structures.

The growth and the chain reaction process are in competition. Whether the growth process completes or the chain reaction starts to take place is determined by which of the two diffusing processes discussed here occurs more easily. A system in which another facet is added to the previous system, shown schematically by the dash-dotted line in Fig. 7 (adding a facet to the lower region is a matter of choice, the same discussion holds) is considered. The two diffusing processes are indicated by the two lines with an arrow. When it is easier for a step-edge atom at the upper site of the lower facet to diffuse across the middle terrace and over the seed and finally incorporate into the lower site of the upper terrace (diffusion process I), then the growth process is completed. On the other hand, if it is easier for the step-edge atom at the upper site of the upper terrace to diffuse across the upper

wide terrace and incorporate into the lower site of the added facet then the chain reaction starts and another seed forms on the adjacent terrace (diffusion process II). Now the problem is which of the two processes takes place. While the probability for the diffusion process I to occur does not depend on the number of steps included in the seed, the probability of the diffusion process II seriously does, and it becomes increasingly difficult for this process to complete as the seeds become larger, because a large seed means more steps to diffuse over, which is a rather stumbling process.

When a seed is small the diffusion process I is dominant, and subsequently the seed grows. However, a turning point exists, and once the seed grows to a certain size, the diffusion process II becomes dominant, and consequently, another seed forms on the adjacent terraces. As a result of these processes, step bunching does not grow infinitely in size, and after it evolves into a particular size its development stops, and also by a by-product, branches are formed that have a tendency to align side by side. These characteristics of this model exactly correspond to the result of experiments.

## V. CONCLUSION

We have experimentally studied how branches, by which we refer to step bunchings that do not run in the substrate miscut direction, emerge and align on the step bunched surface of vicinal GaAs(001) substrates with various miscut directions annealed in AsH<sub>3</sub> and hydrogen. On most of the substrates and for most of the annealing conditions studied in this research, branches were observed, suggesting that they have a relatively low free energy and compose an intrinsic component of this step bunching. The main characteristics of these branches are that they are not randomly distributed on the surface, but have a strong tendency to align side by side, and that on substrates miscut in the group I directions ( $[100]$ ,  $[110]B$ , and  $[110]A$ ) the facets of branches have the azimuth in the group II directions ( $[210]$  and  $[\bar{2}10]$ ), and vice versa. Also the locations where the branches align are not randomly placed on the surface, but are distributed somewhat periodically. These experimental results can be qualitatively understood by the "chain reaction model" we propose in this paper. This model is based on the fact that during annealing, step bunching occurs when an upward net mass transfer across the step edge exists. By considering this net mass transfer on the surface, the evolution of the step bunching can be simulated. Branches emerges simultaneously when a new facet forms. In our model, this newly formed facet grows when its size is small though does not after it reaches a critical size, and instead another new facet forms on the adjacent terrace. By this model we can understand both why the branches have a tendency to align side by side and why the observed step bunching does not grow infinitely in size with annealing time.

<sup>1</sup>L. Hollan and C. Schiller, *J. Cryst. Growth* **22**, 175 (1974).

<sup>2</sup>D. L. Rode, *J. Cryst. Growth* **27**, 313 (1974).

<sup>3</sup>R. H. Saul and D. D. Roccasecca, *J. Appl. Phys.* **44**, 1983 (1973).

<sup>4</sup>T. Kajimura, K. Aiki, and J. Umeda, *Appl. Phys. Lett.* **30**, 526 (1977).

<sup>5</sup>A. J. Derksen, W. J. P. Van Enckevort, and M. S. Couto, *M. J. Phys. D* **27**, 2580 (1994).

<sup>6</sup>M. A. Kulakov, P. Heuell, V. F. Tsvetkov, and B. Bullemer, *Surf. Sci.* **315**, 248 (1994).

<sup>7</sup>Noh-Jung Kwak, In-Hoon Choi, Sung-Wook Lim, and Sang-Hee

- Suh, Korean Appl. Phys. **6**, 532 (1993).
- <sup>8</sup>E. Hahn, H. Schief, V. Marsico, A. Fricke, and K. Kern, Phys. Rev. Lett. **72**, 3378 (1994).
- <sup>9</sup>T. Hashizume, J. E. Rowe, R. A. Malic, K. Motai, K. Cho, J. Kishimoto, and T. Sakurai, J. Vac. Sci. Technol. B **12**, 1809 (1994).
- <sup>10</sup>J. S. Ozcomert, Phys. Rev. Lett. **72**, 258P (1994).
- <sup>11</sup>G. R. Booker, P. C. Klipstein, M. Lakrimi, S. Lyapin, N. J. Mason, R. J. Nicholas, T.-Y. Seong, D. M. Symons, T. A. Vaughan, P. J. Walker, J. Cryst. Growth **145**, 788 (1994).
- <sup>12</sup>X. M. Zhang, D. W. Pashley, I. Kamiya, J. H. Neave, and B. A. Joyce, J. Cryst. Growth **147**, 234 (1995).
- <sup>13</sup>A. Gomyo, H. Hotta, F. Miyasaka, K. Tada, H. Fujii, K. Fukagi, K. Kobayashi, and I. Hino, J. Cryst. Growth **145**, 126 (1994).
- <sup>14</sup>M. Krishnamurthy, A. Lorke, M. Wassermeier, D. R. M. Williams, and P. M. Petroff, J. Vac. Sci. Technol. B **11**, 1384 (1993).
- <sup>15</sup>M. R. Cohen, R. J. Simonson, M. M. Altamirano, K. L. Critchfield, W. T. Kemp, and J. A. Meinhardt, J. Vac. Sci. Technol. A **11**, 971 (1973).
- <sup>16</sup>T. Fukui and H. Saito, Jpn. J. Appl. Phys. **29**, L483 (1990).
- <sup>17</sup>K. Hata, T. Ikoma, H. Hirakawa, T. Okano, A. Kawazu, T. Ueda, and M. Akiyama, J. Appl. Phys. **76**, 5601 (1994).
- <sup>18</sup>K. Hata, H. Hirakawa, T. Okano, T. Ueda, and M. Akiyama, J. Cryst. Growth **160**, 235 (1996).
- <sup>19</sup>K. Hata, K. Hirakawa, T. Okano, T. Ueda, M. Akiyama, Jpn. J. Appl. Phys. **35**, 1280 (1996).
- <sup>20</sup>K. Hata, K. Hirakawa, T. Okano, T. Ueda, and M. Akiyama (unpublished).
- <sup>21</sup>H. C. Abbink, R. M. Broudy, and G. P. McCarthy, J. Appl. Phys. **39**, 4673 (1968).
- <sup>22</sup>J. S. Ozcomert, W. W. Pai, N. C. Bartelt, and J. E. Reutt-Robey, Surf. Sci. **293**, 183 (1993).
- <sup>23</sup>A. V. Latyshev, A. B. Krasilnikov, A. L. Aseev, Surf. Sci. **311**, 395 (1994).
- <sup>24</sup>H. Hibino, T. Fukuda, M. Suzuki, Y. Homma, T. Sato, M. Iwatsuki, K. Miki, and H. Tokumoto, Phys. Rev. B **47**, 13 027 (1993).
- <sup>25</sup>H. Hibino and T. Ogino, Phys. Rev. Lett. **72**, 657 (1994).
- <sup>26</sup>R. J. Phaneuf *et al.*, Phys. Rev. Lett. **71**, 2284 (1993).
- <sup>27</sup>V. Mathet, F. Nguyen-Van-Dau, J. Olivier, and P. J. Galtier, Cryst. Growth **148**, 133 (1995).
- <sup>28</sup>Lian Li, Yi Wei, and I. S. T. Tsong, Surf. Sci. **304**, 1 (1994).
- <sup>29</sup>M. Takeuchi, K. Shiba, K. Sato, H. K. Huang, K. Inoue, and H. Nakashima, Jpn. J. Appl. Phys. **34**, 4411 (1995).
- <sup>30</sup>M. Krishnamurthy, M. Wassermeier, D. R. M. Williams, and P. M. Petroff, Appl. Phys. Lett. **62**, 1922 (1993).
- <sup>31</sup>K. Inoue, K. Kimura, K. Maehashi, S. Hasegawa, M. Iwane, O. Matsuda, and K. Murase, J. Cryst. Growth **127**, 1041 (1993).
- <sup>32</sup>S. Hasegawa, K. Kimura, M. Sato, K. Maehashi, and H. Nakashima, Surf. Sci. **267**, 5 (1992).
- <sup>33</sup>R. Notzel, J. Temmyo, and T. Tamamura, Appl. Phys. Lett. **64**, 3557 (1994).
- <sup>34</sup>R. Notzel, D. Eissler, M. Hohenstein, and K. Ploog, J. Appl. Phys. **74**, 431 (1993).
- <sup>35</sup>R. Notzel, D. Eissler, and K. Ploog, J. Cryst. Growth **127**, 1068 (1993).
- <sup>36</sup>S. L. Skala, S. T. Chou, K. Y. Cheng, J. R. Tucker, and J. W. Lyding, Appl. Phys. Lett. **65**, 722 (1994).
- <sup>37</sup>K. Hata, A. Kawazu, T. Okano, T. Ueda, and M. Akiyama, Appl. Phys. Lett. **63**, 1625 (1993).
- <sup>38</sup>M. Kasu and T. Fukui, Jpn. J. Appl. Phys. **31**, L864 (1992).
- <sup>39</sup>J. Ishizaki, S. Goto, M. Kishida, T. Fukui, and H. Hasegawa, Jpn. J. Appl. Phys. **33**, 721 (1994).
- <sup>40</sup>M. Kasu and N. Kobayashi, Appl. Phys. Lett. **62**, 1262 (1993).
- <sup>41</sup>M. Kasu and N. Kobayashi, Jpn. J. Appl. Phys. **33**, 712 (1994).
- <sup>42</sup>M. Shinohara and N. Inoue, Appl. Phys. Lett. **66**, 1 (1995).
- <sup>43</sup>M. Shinohara, H. Yokoyama, and N. Inoue, J. Vac. Sci. Technol. B **13**, 1773 (1995).
- <sup>44</sup>T. Fukui and H. Saito, Appl. Phys. Lett. **50**, 824 (1987).
- <sup>45</sup>T. Fukui and H. Saito, Jpn. J. Appl. Phys. **29**, L731 (1990).
- <sup>46</sup>T. Fukui and H. Saito, J. Vac. Sci. Technol. B **6**, 1373 (1988).
- <sup>47</sup>H. Saito, K. Uwai, Y. Tokura, and T. Fukui, Appl. Phys. Lett. **63**, 72 (1993).
- <sup>48</sup>F. C. Frank, in *Growth and Perfection of Crystals*, edited by R. Doremus, B. Roberts, and D. Turnbull (Wiley, New York, 1958), p. 411.
- <sup>49</sup>N. Cabrera and D. A. Vermilyea, in *Growth and Perfection of Crystals* (Ref. 48), p. 393.
- <sup>50</sup>J. P. van der Eerden and M. Muller-Krumbharr, Phys. Rev. Lett. **57**, 2431 (1986).
- <sup>51</sup>J. P. van der Eerden and M. Muller-Krumbharr, Phys. Scr. **40**, 337 (1989).
- <sup>52</sup>See for a recent extension of this theory D. Kandel and J. D. Weeks, Phys. Rev. B **49**, 5554 (1994).
- <sup>53</sup>M. D. Pashley and K. W. Haberern, Phys. Rev. Lett. **67**, 2697 (1991).
- <sup>54</sup>M. D. Pashley and K. W. Haberern, Ultramicroscopy **42-44**, 1281 (1992).
- <sup>55</sup>T. Fukui, J. Ishizaki, S. Hara, J. Motohisa, and H. Hasegawa, J. Cryst. Growth **146**, 183 (1995).
- <sup>56</sup>M. Suzuki, Y. Kidoh, Y. Homma, and R. Kaneko, Appl. Phys. Lett. **58**, 2225 (1991).
- <sup>57</sup>G. W. Smith, A. J. Pidduck, C. R. Whitehouse, J. L. Gasper, A. M. Keir, and C. Pickering, Appl. Phys. Lett. **59**, 3282 (1991).
- <sup>58</sup>C. R. Whitehouse (unpublished).
- <sup>59</sup>H. Benisty, E. Bockenhoff, and A. Taineau, Appl. Phys. Lett. **60**, 1987 (1992).
- <sup>60</sup>C. Herring, Phys. Rev. **82**, 87 (1951).
- <sup>61</sup>E. Bockenhoff and H. Benisty, J. Cryst. Growth **114**, 619 (1991).
- <sup>62</sup>G. H. Olsen, T. J. Zamerowski, and F. Z. Hawrylo, J. Cryst. Growth **59**, 654 (1982).
- <sup>63</sup>A. Madhukar, K. C. Rajkumar, and P. Chen, Appl. Phys. Lett. **62**, 1547 (1993).
- <sup>64</sup>R. Nozel *et al.*, Phys. Rev. B **45**, 3507 (1992).
- <sup>65</sup>Min-Suk Lee, Y. Kim, K. Moo-Song, K. Seong-II, M. Suk-ki, Y. D. Kim, and S. Nahm, Appl. Phys. Lett. **63**, 3052 (1993).
- <sup>66</sup>R. Notzel, J. Temmyo, and T. Tamamura, Appl. Phys. Lett. **64**, 3557 (1994).
- <sup>67</sup>T. Fukui and S. Ando, Jpn. J. Appl. Phys. **29**, 731 (1990).
- <sup>68</sup>M. D. Pashley, Phys. Rev. B **40**, 10 481 (1981).
- <sup>69</sup>E. J. Heller, Z. Y. Zhang, and M. G. Lagally, Phys. Rev. Lett. **71**, 743 (1993).
- <sup>70</sup>K. Ohkuri, J. Ishizaki, S. Hara, and T. Fukui, J. Cryst. Growth **160**, 235 (1996).
- <sup>71</sup>K. Hata, H. Shigekawa, and T. Okano (unpublished).
- <sup>72</sup>R. L. Schwoebel and E. J. Shipsey, J. Appl. Phys. **37**, 3682 (1966).